Journal of Power Sources 270 (2014) 92–100

Contents lists available at ScienceDirect

Journal of Power Sources

journal homepage: www.elsevier.com/locate/jpowsour

Influence of overcharge and over-discharge on the impedance response of $LiCoO_2$|C batteries

Salim Erol [a], Mark E. Orazem [a, *], Richard P. Muller [b]

[a] Department of Chemical Engineering, University of Florida, Gainesville, FL 32611, USA
[b] Sandia National Laboratories, Albuquerque, NM 87185-1322, USA

HIGHLIGHTS

- Impedance analysis of Li-ion battery at various states-of-charge.
- Novel application of measurement model to Li-ion battery.
- Interpretation of impedance response of an overcharged and over-discharged Li-ion battery.
- Explanation of some failure mechanisms of a Li-ion battery.

ARTICLE INFO

Article history:
Received 28 May 2014
Received in revised form
2 July 2014
Accepted 7 July 2014
Available online 17 July 2014

Keywords:
Overcharge
Over-discharge
Capacity loss
Self-charge
Self-discharge
Impedance spectroscopy

ABSTRACT

This paper provides the results of impedance measurements on commercially available $LiCoO_2$|C coin-type cells. The impedance response was shown to be extremely sensitive to state-of-charge, over-charge, and over-discharge. Interestingly, the impedance showed a persistent change to the electrochemical characteristics of a coin cell subject to overcharge; whereas, the electrochemical characteristics returned to normal for a coin cell subject to over-discharge. A measurement model analysis was used to show the reversibility of the impedance behavior of an over-discharged cell and the irreversibility of the impedance response of an overcharged cell.

1. Introduction

Li-ion batteries are rechargeable batteries that are frequently used as power sources for household and industrial applications because they have a higher energy and power density as compared to other batteries such as nickel–cadmium and lead-acid. The most common Li-ion batteries use a $LiCoO_2$ cathode, a graphite anode, and a non-aqueous electrolyte composed of lithium salt such as $LiPF_6$ in a mixture of organic solvents such as ethylene carbonate, propylene carbonate, dimethyl carbonate, and diethyl carbonate [1,2].

The cycle life and capacity of a Li-ion battery are reduced if it is overcharged or in some cases over-discharged. Kise et al. [3] measured the impedance at different temperatures of a Li-ion cell under its normal range of potential and tested the internal temperature of an overcharged cell. They did not indicate impedance growth while overcharging the battery. Li et al. [4] used impedance to compare cycling effects between uncoated $LiCoO_2$ and $FePO_4$-coated $LiCoO_2$ cathode materials. They showed temperature profiles while overcharging these batteries and mentioned thermal runaway for the uncoated $LiCoO_2$ cathode. Maleki and Howard [5] reported that over-discharging of Li-ion cells below 1.5 V may cause capacity losses and/or thermal stability changes which could impact tolerance to abuse conditions. They reported impedance diagrams which showed increases in high and low frequency asymptotes with cycle life. Chen et al. [6] determined the conductivity of a lithium secondary battery for different state-of-charge conditions using impedance spectroscopy. They added an aromatic monomer that is electropolymerized during overcharging the battery to the electrolyte. The insulating polymer film protected the battery from overcharging. Belov and Yang [7] used electrical impedance spectroscopy and scanning electron microscopy to

* Corresponding author.
E-mail address: meo@che.ufl.edu (M.E. Orazem).

http://dx.doi.org/10.1016/j.jpowsour.2014.07.038
0378-7753/

characterize electrode materials at different state-of-overcharge conditions. A dramatic increase in resistance for the 4.6 and 5.0 V test was reported, but the interpretation was qualitative. Love and Swider-Lyons [8] used the impedance spectroscopy technique to diagnose overcharged $LiCoO_2$|C prismatic cells. They measured impedances while gradually overcharging and discharging the battery. They showed that a single 4.6 V overcharge shows clear differentiation in the impedance values at 500 Hz, and proposed that a single-frequency impedance measurement at 500 Hz provides a simple means of monitoring battery health.

The object of the present work is to explore the influence of overcharge and over-discharge conditions on the impedance response of commercial $LiCoO_2$|C batteries. Superposition of impedance spectra, made possible by application of a measurement model analysis, facilitated interpretation of the impedance responses associated with abuse conditions of Li-ion batteries.

2. Experimental method

Electrochemical experiments were performed on commercial $LiCoO_2$|C coin cells. Impedance spectroscopy was used to monitor changes associated with different states-of-charge, imposition of overcharge, and imposition of over-discharge.

2.1. Materials

Commercial secondary LIR2032 button (or coin) cells were purchased from AA Portable Power Corp. (Richmond, CA, www.batteryspace.com). LIR refers to Lithium-ion rechargeable, and the 2032 specification means that the batteries were 20 mm in diameter and 3.2 mm in height. The cathode was $LiCoO_2$, the separator was Celgard 8 μm and the anode was carbon. The normal operating potential range of the cells reported by the supplier [9], between 3.00 V (0% state-of-charge) and 4.20 V (100% state-of-charge), is in agreement with published literature [10–12].

2.2. Instrumentation

Electrochemical experiments and impedance measurements were performed using a Gamry PCI4/750 Potentiostat connected to a desktop computer. Gamry's Virtual Front Panel (VFP600) and Electrochemical Impedance Spectroscopy (EIS300) software packages were used to run the experiments. The primary purpose of the potentiostat in these experiments was to maintain a constant cell potential while measuring the impedance.

2.3. Protocol

Following the previous work [13], the impedance response was analyzed throughout the normal potential range under charge and discharge profiles. The impedance was also analyzed under overcharge and over-discharge conditions. Capacity measurements were used to show the extent to which the overcharging and over-discharging processes affected battery performance.

As received, the $LiCoO_2$|C cells had an open-circuit potential of 3.8 ± 0.2 V. The cells were slowly charged to 4.20 V under galvanostatic control at a current of 2 mA. To assess the capacity of the battery, each cell was subsequently discharged to 3 V at a constant 30 mA current (the nominal 1C discharge rate) and charged back to 4.20 V with the same constant 30 mA current. During charge or discharge throughout the normal range, the capacity was obtained by multiplying the amount of applied current with the time elapsed. The average measured value for the capacity of the LIR2032 battery at 1C rate was 30 mAh, in agreement with the vendor documentation [9,14].

For impedance measurements in the normal potential range, the cells were held for at least one hour at a constant cell potential of 4.20 V. After the constant-potential rest period, the impedance was measured using a 10 mV perturbation and 100 kHz–20 mHz frequency range. The linear response of low-frequency Lissajous plots was used to ensure linearity during the impedance measurement [15]. Three replicated impedance scans were obtained for each condition tested. Following impedance measurements at a given potential, the cell potential was modified for the discharge profile in 0.20 V increments down to and including 3.00 V. The change in potential was conducted galvanostatically at a 2 mA current. For each potential step, the battery was allowed to stabilize for a period of one hour, in which the current was reduced to a value that was smaller than 0.02 mA. Impedance measurements were made in triplicate following stabilization at the desired potential. The charge profile, following the same procedure, was executed immediately up to and including 4.20 V.

The effect of overcharging and over-discharging a $LiCoO_2$|C cell was also analyzed. To assess the influence of overcharging the battery, the cell was initially charged under constant 2 mA current to 4.20 V. Impedance measurements were performed at each 0.08 V step up to and including 5.00 V. As before, a 10 mV ac perturbation and 100 kHz–20 mHz frequency range were implemented. A similar protocol was followed for the over-discharge. Another cell was initially discharged under constant current to 3.00 V. Impedance measurements were performed at each 0.08 V step down to and including 2.20 V. Capacity measurements, using constant 30 mA current for both charging and discharging, were obtained before and after the overcharge and over-discharge protocols to quantify changes in battery performance.

All experiments were performed at room temperature (around 20 °C), and they were repeated 3–4 times with same type of battery to ensure that the results were both consistent and reproducible. The software incorporated in the Gamry system enabled consistent and precise procedures to be performed which served to reduce errors among the repetitive experiments.

3. Results and discussion

The impedance response of the $LiCoO_2$|C coin cells is presented for state-of-charge, overcharge, and over-discharge conditions.

3.1. State-of-charge

The impedance response for a commercial $LiCoO_2$|C coin cells is presented in Fig. 1 with cell potential from 3 to 4.2 V as a parameter. These results represent the impedance response under normal operating conditions and under the discharge profile. Results obtained under the charge profile were identical. Notably, the impedance was significantly larger at 3 V, especially at the low frequencies, even though it became smaller while the potential approached to the upper limit in the normal operating range for the $LiCoO_2$|C coin cell. While many factors contribute to selection of the operational potential range of a battery, the impedance results suggest that 3.2 V would be a more appropriate lower limit for the normal potential range.

3.2. Overcharge

The impedance is a strong function of cell potential. To explore the sensitivity of impedance spectroscopy for overcharging the battery, the coin cell potential was increased in 80 mV increments starting from 4.2 V and the impedance was measured after the cell current approached zero, i.e., 0.02 mA. To make the features visible,

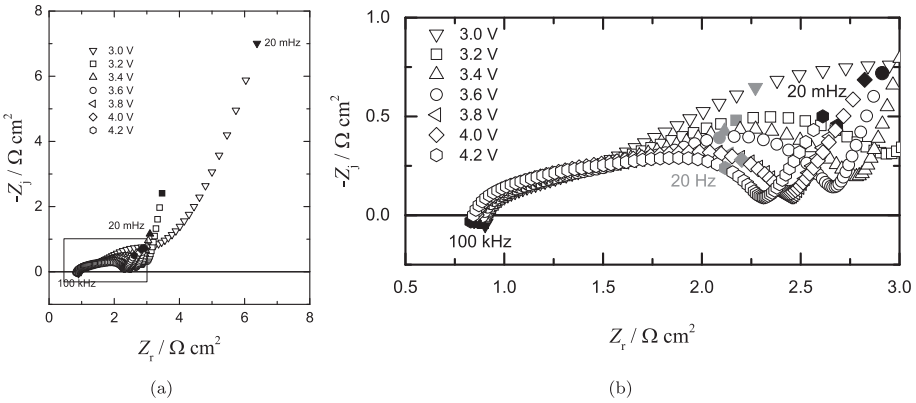

Fig. 1. Impedance response in Nyquist format for a $LiCoO_2$|C coin cell under normal operating conditions with cell potential as a parameter: a) complete spectra and b) low impedance values corresponding to the box in (a). The impedance was measured under the discharge profile. Results obtained under the charge profile were identical.

the impedance response is presented in a sequence of plots. The impedance response is presented in Fig. 2 for cell potential ranging from 4.20 to 4.44 V (Fig. 2(a)) and potential ranging from 4.44 to 4.60 V (Fig. 2(b)). The impedance at potentials from 3.2 to 4.52 V were almost identical. While many factors contribute to selection of the operational potential range of a battery, this superposition of impedance diagrams suggests that an upper value for the normal operating range could be 4.5 V. The impedance at 4.6 V is strikingly different, in agreement with the results reported by Belov and Yang [7] and Love and Swider-Lyons [8].

The impedance values grew dramatically from a potential of 4.60 V to 4.76 V, as shown in Fig. 3. In Fig. 3(a), a substantial growth in the low-frequency impedance is seen for the transition from 4.6 V to 4.76 V. The zoomed image in Fig. 3(b) indicates comparatively smaller amount of differences in the high-frequency response.

The impedance response is presented in Fig. 4 for potentials ranging from 4.76 to 5.00 V. In contrast to the results presented in Fig. 3, a capacitive loop is evident at low frequencies for cell potentials above 4.92 V. In addition, as seen in the zoomed image in Fig. 4(b), the size of the capacitive loop at high frequencies increases with potential for potentials greater than 4.76 V.

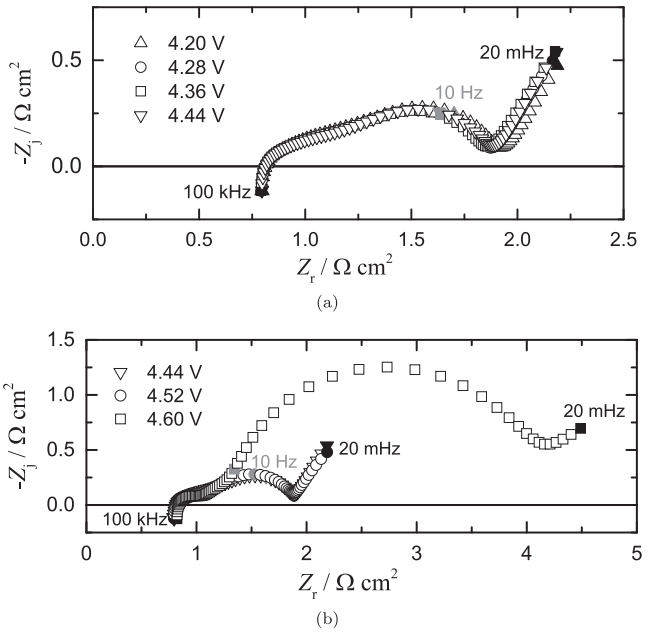

Fig. 2. Impedance response in Nyquist format for a $LiCoO_2$|C coin cell under overcharge conditions with cell potential as a parameter: a) potential ranging from 4.20 to 4.44 V; and b) potential ranging from 4.44 to 4.60 V.

After overcharging to a potential of 5 V, the battery was allowed to relax for two days at the open-circuit condition. When held at open-circuit, the potential of the overcharged battery rapidly decreased for the first two hours and then slowly approached the normal operating range for the rest of the time, as shown in Fig. 5.

During self-discharge after overcharging to 5 V, impedance measurements were collected as a function of time to show the evolution of the impedance response during the self-discharge. The results given in Fig. 6 show that the impedance increased as the cell potential approached values within the normal operating range. The major change was seen in the low-frequency part of the spectrum as revealed in Fig. 6(a). The zoomed image shown in Fig. 6(b) reveals that the high-frequency capacitive loop did not change very much.

After the self-discharge period, the overcharged battery was discharged to 4 V, a potential within the normal range. A dramatic difference on the impedance between a pristine cell and an overcharged cell is seen in Fig. 7. Both high-frequency capacitive loops and the low-frequency parts of the impedance responses are distinctly altered.

The capacity results for before and after overcharging the cell are presented in Fig. 8. For both the pristine and overcharged cells, the capacity measurements were made at a relatively large 1C rate after only one charge–discharge cycle. Thus, the capacity on discharge at a fixed 30 mA rate was larger than it was during the subsequent charge. According to Buiel and Dahn [16], this difference may be attributed to the consumption of lithium ions by reactions that increase the SEI layer thickness. The capacity difference between the pristine and overcharged batteries at both the fully-charged and fully-discharged condition was roughly 4.5 mAh, which corresponds to a 15% capacity loss at the end of the discharge step and a 20% capacity loss at the conclusion of the charge step.

3.3. Over-discharge

The cell potential was decreased in 80 mV increments starting from 3 V, and the impedance was measured after the cell current approached zero to explore the sensitivity of impedance spectroscopy to over-discharging the battery. The impedance was again a strong function of cell potential as observed in the overcharging case. The impedance response is presented in Fig. 9 for cell potential ranging from 3.00 to 2.84 V. The zoomed image in Fig. 9(b) reveals that the high-frequency loop disappeared as the battery

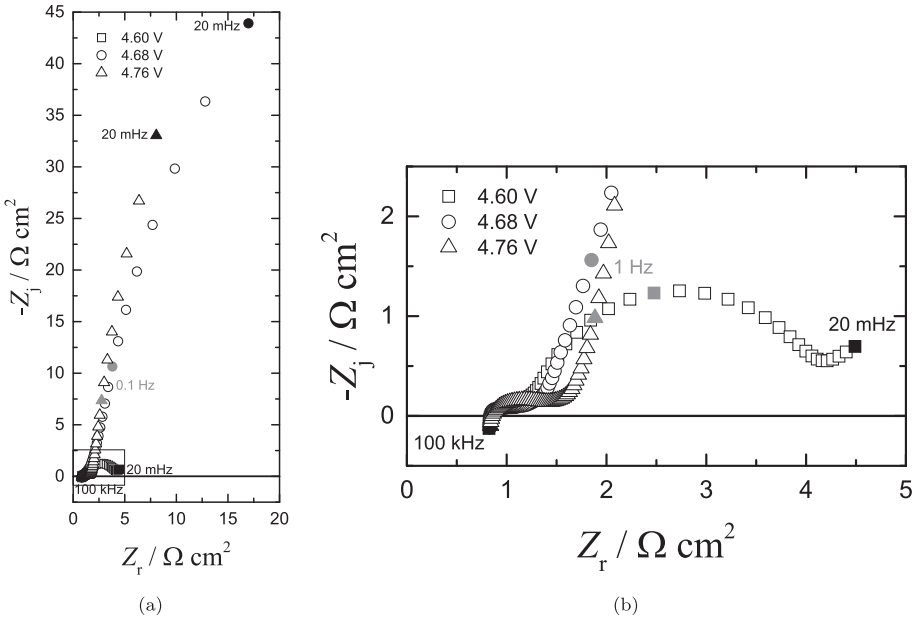

Fig. 3. Impedance response in Nyquist format for a $LiCoO_2$|C coin cell under overcharge conditions with cell potential, ranging from 4.60 to 4.76 V, as a parameter: a) complete spectra and b) smaller impedance values corresponding to the box in (a).

was subjected to over-discharge. The impedance response is presented in Fig. 10 for cell potential ranging from 2.84 to 2.60 V (Fig. 10(a)), potential ranging from 2.60 to 2.36 V (Fig. 10(b)), and potential ranging from 2.36 to 2.20 V (Fig. 10(c)). High-frequency results are not shown in these figures since most of the change in the impedance at different potentials came from the low-frequency part. The low-frequency part of the impedance response became larger as the cell potential decreased under over-discharge conditions.

After over-discharging to a potential of 2.20 V, the battery was allowed to relax for two days at the open-circuit condition. When held at open-circuit, the over-discharged battery slowly reached a cell potential within the normal operating range, as shown in Fig. 11.

During self-charge after over-discharging to 2.2 V, impedance measurements were collected as a function of time to show the evolution of the impedance response during the self-charge. The results are shown in Fig. 12. The impedance increased over the first 3 h and then began to decrease for the measurement taken at 5 h. After 48 h, the impedance was similar to that obtained before the potential excursion.

The impedance response and capacity measured before and after the cell was over-discharged are presented in Figs. 13 and 14, respectively. The results are in striking contrast to the results seen for the overcharged battery (Figs. 7 and 8). Minor differences at the capacity (presumably due to the cycling) and the impedance (due to only ohmic resistance) are observed in these results. It should be noted, however, that Maleki and Howard [5] over-discharged the

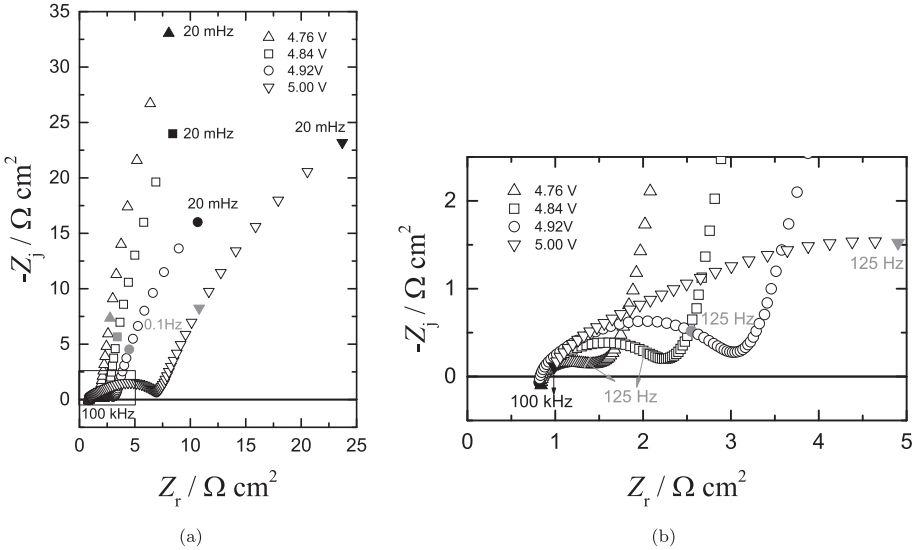

Fig. 4. Impedance response in Nyquist format for a $LiCoO_2$|C coin cell under overcharge conditions with cell potential, ranging from 4.76 to 5.00 V, as a parameter: a) complete spectra and b) high frequency values corresponding to the box in (a).

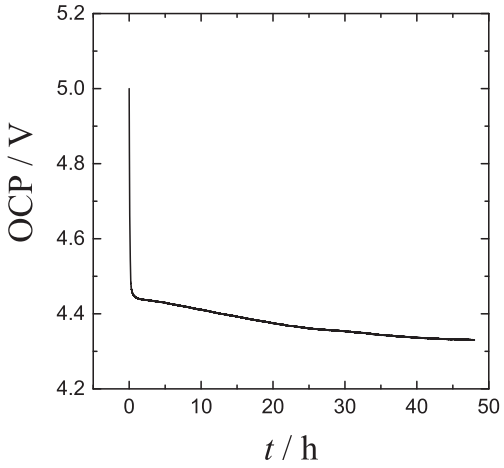

Fig. 5. Open-circuit potential as a function of time for an overcharged $LiCoO_2$|C coin cell.

Li-ion batteries to lower potentials and observed a capacity fade for the batteries.

4. Measurement model analysis

A measurement model analysis was employed to extract physically meaningful parameters. A graphical analysis was used to show that the change in the impedance response with over-discharging was due to a change in the ohmic resistance.

4.1. Measurement model

The measurement model method for distinguishing between bias and stochastic errors is based on using a generalized model as a filter for non-replicacy of impedance data. [17] The measurement model is composed of a superposition of line-shapes that can be

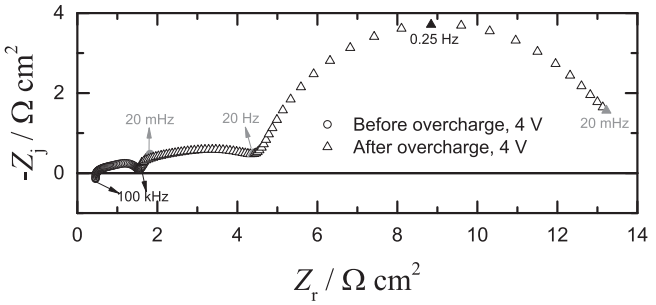

Fig. 7. Impedance response of a $LiCoO_2$|C coin cell at a potential of 4 V before and after the cell was overcharged.

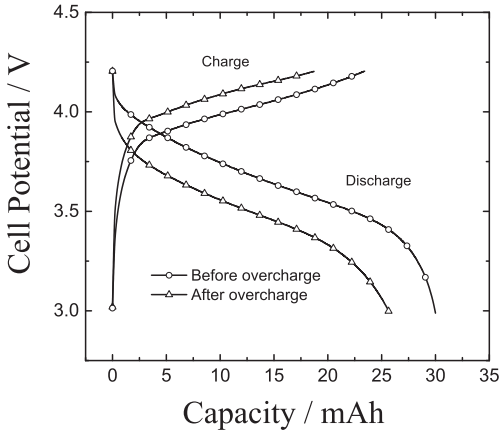

Fig. 8. Discharge and charge capacity of a $LiCoO_2$|C coin cell before and after the cell was overcharged. Symbols used to distinguish lines are placed at an interval of 20 measurements.

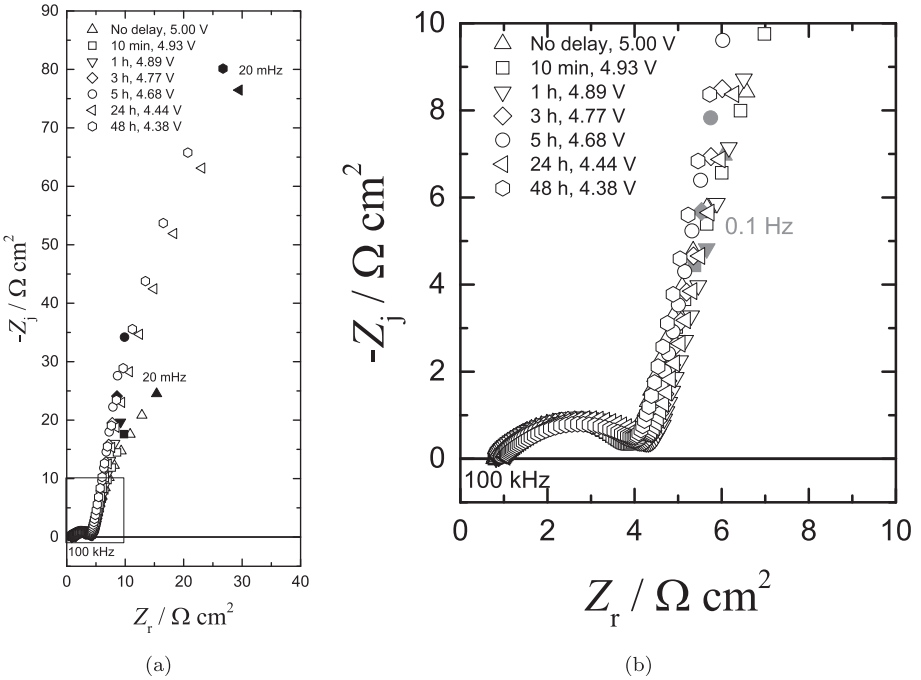

Fig. 6. Impedance response in Nyquist format for a $LiCoO_2$|C coin cell during self-discharge under overcharge conditions with elapsed time as a parameter; a) complete spectra and b) high frequency values corresponding to the box in (a).

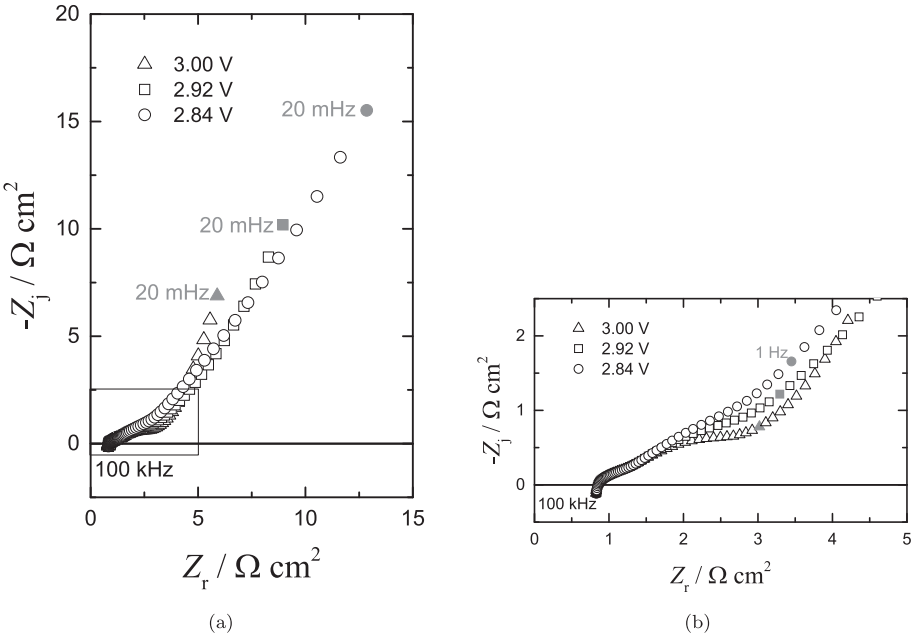

Fig. 9. Impedance response in Nyquist format for a $LiCoO_2$|C coin cell under over-discharge conditions with cell potential, ranging from 3.00 to 2.84 V, as a parameter: a) complete spectra and b) high frequency values corresponding to the box in (a).

arbitrarily chosen subject to the constraint that the model satisfies the Kramers–Kronig relations. The model composed of Voigt elements in series with a solution resistance, shown in Fig. 15 and described mathematically by.

$$Z = R_0 + \sum_{k=1}^{K} \frac{R_k}{1 + j\omega\tau_k} \quad (1)$$

has been shown to be a useful measurement model. With a sufficient number of parameters, the Voigt model was able to provide a statistically significant fit to a broad variety of impedance spectra. [18]

The measurement model is used first to filter lack of replication of repeated impedance scans. The statistics of the residual errors yields an estimate for the variance (or standard deviation) of stochastic measurement errors. [19] This experimentally-determined variance is then used to weight subsequent regression of the measurement model to determine consistency with the Kramers–Kronig relations. [20,21] If the data can be represented by a model that is itself consistent with the Kramers–Kronig relations, the data can be considered to be consistent. The use of an

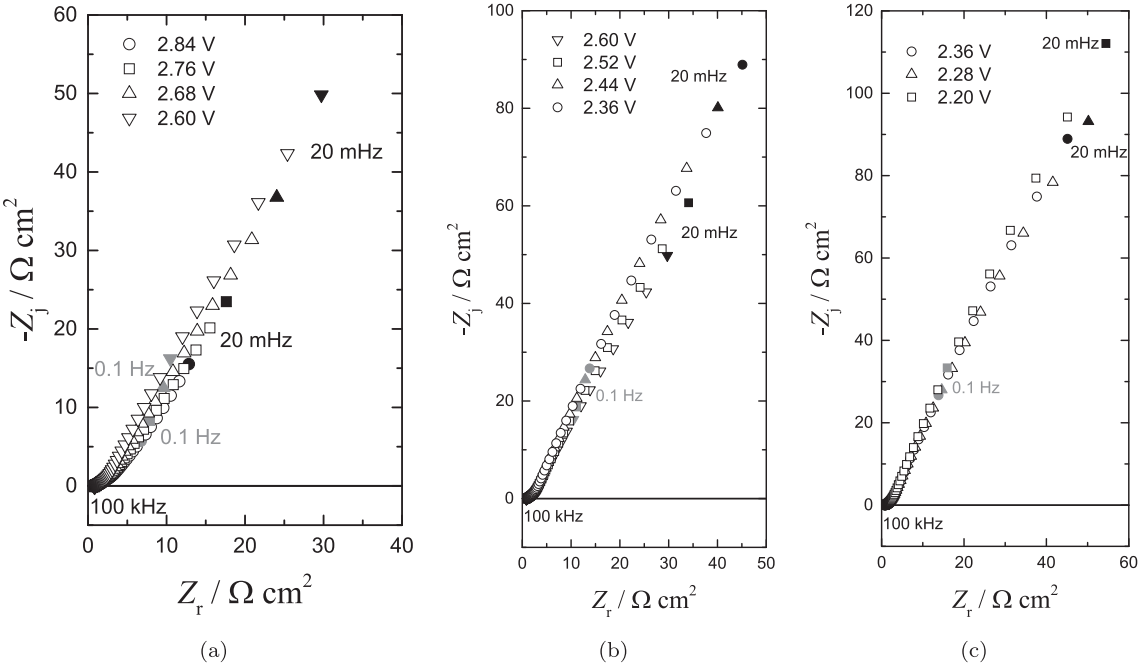

Fig. 10. Impedance response in Nyquist format for a $LiCoO_2$|C coin cell under over-discharge conditions with cell potential as a parameter: a) potential ranging from 2.84 to 2.60 V; b) potential ranging from 2.60 to 2.36 V, and c) potential ranging from 2.36 to 2.20 V.

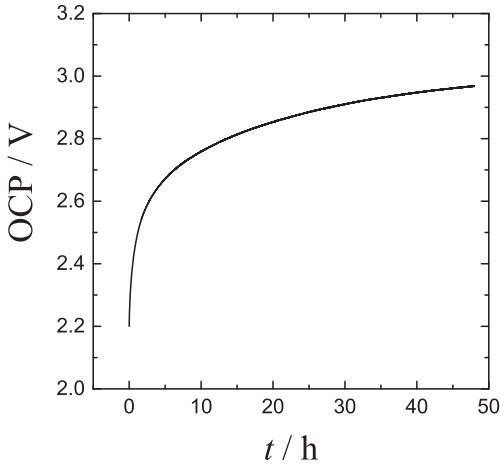

Fig. 11. Open-circuit potential as a function of time for an over-discharged $LiCoO_2$|C coin cell.

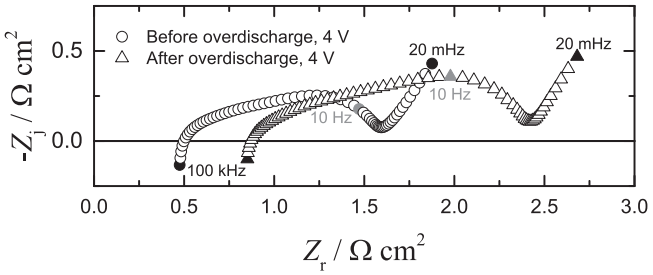

Fig. 13. Impedance response of a $LiCoO_2$|C coin cell at a potential of 4 V before and after the cell was over-discharged.

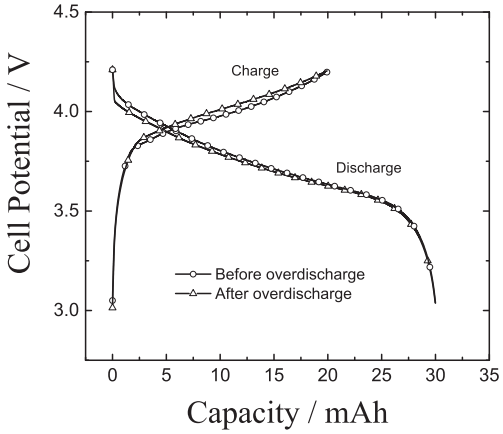

Fig. 14. Discharge and charge capacity of a $LiCoO_2$|C coin cell before and after the cell was over-discharged. Symbols used to distinguish lines are placed at an interval of 20 measurements.

experimental determination of the stochastic error structure allows formal quantification of the extent of agreement with the Kramers–Kronig relations.

4.2. Measurement model results

The error analysis approach was applied to electrochemical impedance data collected for the Li-ion batteries. The experimental data was evaluated for the consistency with the Kramers–Kronig relations, using the experimentally determined variance to weight the regression of the measurement model. For measurements at normal operating potentials, the results at frequencies higher than 25 kHz were found to be inconsistent with the Kramers–Kronig relations. For the system subjected to overcharge to 5 V, subsequent measurements at a lower voltage were consistent with the Kramers–Kronig relations, even at frequencies as high as 100 kHz. In all cases, the data collected at low frequencies (20 mHz) were found to be consistent with the Kramers–Kronig relations. This result was observed for systems undergoing obvious transient behavior, such as shown in Figs. 6 and 12. The consistency of the low-frequency data with the Kramers–Kronig relations means that the system was changing sufficiently slowly that individual scans could be

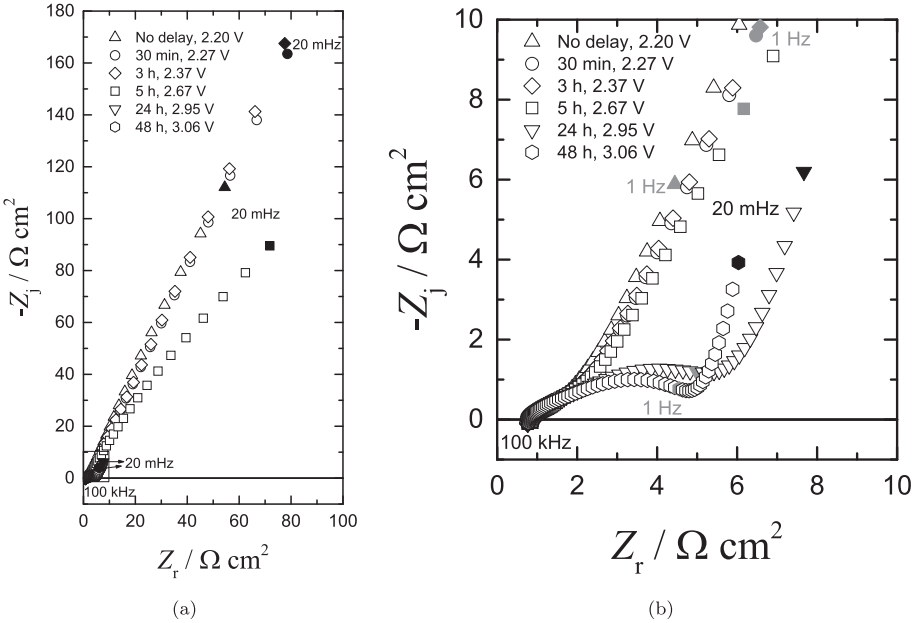

Fig. 12. Impedance response in Nyquist format for a $LiCoO_2$|C coin cell during self-charge under over-discharge conditions with elapsed time as a parameter; a) complete spectra and b) high frequency values corresponding to the box in (a).

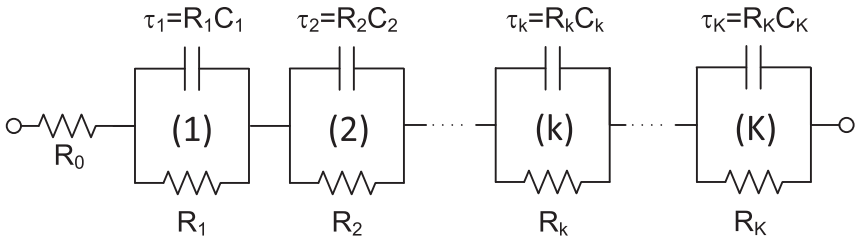

Fig. 15. A schematic representation of the measurement model used by Agarwal et al. [18–20].

regarded as being stationary. Only the Kramers–Kronig-consistent data were used for subsequent analysis under the assumption that the truncated data were subject to artifact such as caused by wires or electronics.

Comparison of scaled impedance may be used to assess to the extent to which differences in impedance response may be attributed to changes in reaction chemistry. This approach was used successfully by Baril et al. [22] to show that the temporal evolution of impedance for a magnesium alloy could be attributed to changes in coverage by an oxide layer rather than to changes in reaction chemistry. The use of scaled impedance requires robust estimates for the ohmic resistance and the zero-frequency asymptote. In the present case, the scaling was based on the size of the high-frequency capacitive loop. The measurement model was used to assess the high-frequency asymptote for the real part of the impedance. This term is the ohmic resistance (R_e) for the cell. A truncated data set was used to estimate the charge-transfer resistance (R_t) for the high-frequency capacitive loop. The concept of using the measurement model to identify limits was presented by Orazem et al. [23] for estimating the polarization resistance in corrosion studies.

The effect of overcharging and over-discharging can be demonstrated by plotting a scaled impedance in which $-Z_j/R_t$ is plotted as a function of $(Z_r-R_e)/R_t$. The results are presented in Fig. 16(a). Superposition of the scaled data was not possible,

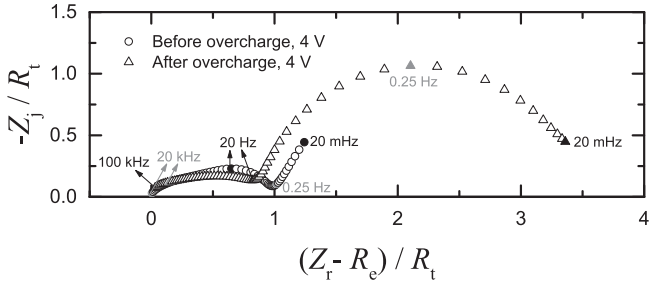

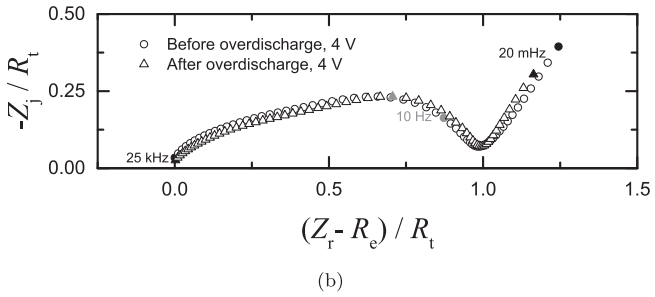

Fig. 16. Scaled impedance result of a $LiCoO_2$|C cell at 4 V; a) before and after the cell was overcharged (see Fig. 7) and b) before and after the cell was over-discharged (see Fig. 13).

suggesting that the chemistry of the battery changed after overcharging. In contrast, as shown in Fig. 16(b), superposition was possible for scaled impedance results before and after over-discharge. The superposition of impedance curves shows that there were no mechanistic changes caused by over-discharge to a particular potential, for this case 2.2 V. The change in the impedance response after over-discharge can be attributed solely to a change in the ohmic resistance.

The results of the overcharge experiments suggest, in agreement with of Amatucci et al. [24], that some of the Li^+ ions in the $LiCoO_2$ cathode are required to maintain the proper structural stability and oxidation state of the CoO_2 lattice. Under overcharge, these are removed, resulting in either a phase transition to a different CoO_2 morphology or breaking bonds that never properly heal. The observation that the voltage recovers (Fig. 5), but not the impedance (Fig. 16(a)), may be attributed to the sensitivity of impedance to transport and kinetic limitations.

The over-discharge results imply a source for extra Li^+ ions, which may be the SEI layer at the anode/electrolyte interface. This hypothesis is consistent with the transient change in the impedance. The observation that the open-circuit potential (Fig. 11) and impedance response from the layer (Fig. 16(b)) recovered under open-circuit conditions is notable, as this healing occurred without cell cycling. It is possible that the lowest value of over-discharge potential in the present work was not sufficiently low to cause irreversible damage. Maleki and Howard [5] over-discharged the Li-ion batteries to lower potentials and observed a capacity fade for their batteries.

5. Conclusions

Impedance spectroscopy is shown to be very sensitive to the condition and the history of the Li-ion battery. The magnitude of the impedance increased tremendously when the battery is either overcharged or over-discharged. After being overcharged, the battery returned to a potential that was well within normal potential range, but the impedance remained large. This has consequences for managing the state-of-charge of a battery stack. A battery stack is charged or discharged with whole batteries which are serially connected. Therefore, overcharge might occur for some batteries in the stack while charging. This work supports the use of impedance spectroscopy as a diagnostic tool to detect imbalances of charging conditions for individual cells in a stack.

The concept of scaled impedance was shown to be useful for correlating the impedance before and after over-discharge. The ability to superimpose scaled impedance in Nyquist plots provided evidence that the reaction chemistry was unchanged by over-discharge. The measurement model, originally developed to assess the stochastic and bias error structure of impedance data, was used to identify low and high-frequency limits of the capacitive loop needed to scale the impedance.

This work provides a guidance for the development of interpretation models for the impedance of Li-ion batteries. The

influence of overcharge on the battery is envisioned to influence the low-frequency response. A model using a formulation based on electrochemical reaction kinetics and anomalous diffusion is presented in a subsequent paper.

Acknowledgments

This work was supported by the Laboratory Directed Research and Development Program at Sandia National Laboratories. Sandia is a multi-program laboratory operated for the U.S. DOE NNSA under contract DE-AC04-94AL85000. Erol acknowledges a fellowship from the government of Turkey.

References

[1] M. Winter, R.J. Brodd, Chem. Rev. 104 (10) (2004) 4245–4270.
[2] K. Ozawa (Ed.), Lithium Ion Rechargeable Batteries: Materials, Technology, and New Applications, Wiley-VCH Verlag GmbH & Co, 2009.
[3] M. Kise, S. Yoshioka, K. Hamano, H. Kuriki, T. Nishimura, H. Urushibata, J. Electrochem. Soc. 153 (2006) A1004–A1011.
[4] G. Li, Z. Yang, W. Yang, J. Power Sources 183 (2008) 741–748.
[5] H. Maleki, J.N. Howard, J. Power Sources 160 (2006) 1395–1402.
[6] G. Chen, K.E. Thomas-Alyea, J. Newman, T.J. Richardson, Electrochim. Acta 50 (2005) 4666–4673.
[7] D. Belov, M.-H. Yang, J. Solid State Electrochem. 12 (2008) 885–894.
[8] C. Love, K. Swider-Lyons, Electrochem. Solid State Lett. 15 (4) (2012) A53–A56.
[9] Rechargeable Li-ion Button Battery Serial LIR2032, http://www.batteryspace.com/productimages/aa/20060224/LIR2032_new1.pdf, (accessed 03.08.14).
[10] P. Ramadass, B. Haran, R. White, B.N. Popov, J. Power Sources 111 (2002) 210–220.
[11] S. Tintignac, R. Baddour-Hadjeana, J.-P. Pereira-Ramosa, R. Salotb, Electrochim. Acta 60 (2012) 121–129.
[12] S. Watanabe, M. Kinoshita, K. Nakura, J. Power Sources 247 (2014) 412–422.
[13] S. Erol, Electrochemical Impedance Analysis of Lithium Cobalt Oxide Batteries, Master's thesis, University of Florida, 2011.
[14] Powerstream Li-ion Coin Cell Lir2032 data sheet, http://www.powerstream.com/p/Lir2032.pdf, (accessed 03.08.14).
[15] B. Hirschorn, B. Tribollet, M.E. Orazem, Israel J. Chem. 48 (2008) 133–142.
[16] E. Buiel, J. Dahn, Electrochim. Acta 45 (1999) 121–130.
[17] M.E. Orazem, J. Electroanal. Chem. 572 (2004) 317–327.
[18] P. Agarwal, M.E. Orazem, L.H. García-Rubio, J. Electrochem. Soc. 139 (7) (1992) 1917–1927.
[19] P. Agarwal, O.D. Crisalle, M.E. Orazem, L.H. García-Rubio, J. Electrochem. Soc. 142 (1995) 4149–4158.
[20] P. Agarwal, M.E. Orazem, L.H. García-Rubio, J. Electrochem. Soc. 142 (1995) 4159–4168.
[21] P. Agarwal, M.E. Orazem, L.H. García-Rubio, Application of the kramers kronig relations to electrochemical impedance spectroscopy, in: J. Scully, D. Silverman, M. Kendig (Eds.), Electrochemical Impedance: Analysis and Interpretation, America Society for Testing and Materials, Philadelphia, PA, 1993, pp. 115–139. Vol. ASTM STP 1188.
[22] G. Baril, G. Galicia, C. Deslouis, N. Pèbére, B. Tribollet, V. Vivier, J. Electrochem. Soc. 154 (2007) C108–C113.
[23] M.E. Orazem, P.T. Wojcik, M. Durbha, I. Frateur, L.H. García-Rubio, Mat. Sci. Forum 289–292 (1998) 813–828.
[24] G.G. Amatucci, J.M. Tarascon, L.C. Klein, J. Electrochem. Soc. 143 (1996) 1114–1123.